FEBS Letters 588 (2014) 1715–1719

journal homepage: www.FEBSLetters.org

Functional relevance of the internal hydrophobic cavity of urate oxidase

Nathalie Colloc'h [a,b,c,*], Thierry Prangé [d]

[a] CERVoxy Team, ISTCT UMR 6301, CNRS, Centre Cyceron, Caen, France
[b] ISTCT UMR 6301, CEA, DSV/I2BM, Caen, France
[c] ISTCT UMR 6301, Université de Caen Basse-Normandie, Normandie Université, Caen, France
[d] LCRB UMR 8015, CNRS, Université Paris Descartes, Faculté de Pharmacie, 4 Avenue de l'Observatoire, 75006 Paris, France

ARTICLE INFO

Article history:
Received 18 December 2013
Revised 10 March 2014
Accepted 10 March 2014
Available online 18 March 2014

Edited by Miguel De la Rosa

Keywords:
Uricase
X-ray diffraction
Cavity plasticity
High pressure
Inert gas
Oxygen pressure

ABSTRACT

Urate oxidase from *Aspergillus flavus* is a 135 kDa homo-tetramer which has a hydrophobic cavity buried within each monomer and located close to its active site. Crystallographic studies under moderate gas pressure and high hydrostatic pressure have shown that both gas presence and high pressure would rigidify the cavity leading to an inhibition of the catalytic activity. Analysis of the cavity volume variations and functional modifications suggest that the flexibility of the cavity would be an essential parameter for the active site efficiency. This cavity would act as a connecting vessel to give flexibility to the neighboring active site, and its expansion under pure oxygen pressure reveals that it might serve as a transient reservoir on its pathway to the active site.

1. Introduction

Urate oxidase (uricase; EC 1.7.3.3; UOX) is a tetrameric enzyme belonging to the purine degradation pathway which catalyzes the oxidation of uric acid (1) to a metastable intermediate, 5-hydroxy-isourate (5-HIU) (2). The reaction needs molecular oxygen and releases hydrogen peroxide. 5-HIU is further transformed to S-allantoin (3) through a catalytic cascade.

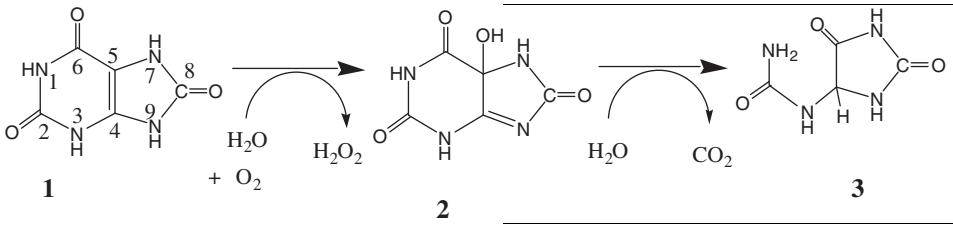

The exact catalytic mechanism is still not fully understood, there is no cofactor nor metallic ion, the optimal pH is basic (between 8.5 and 9), and it is known for a long time that the oxygen atoms in H_2O_2 derive from those of O_2 [1–5].

UOX from *Aspergillus flavus* in presence of a competitive inhibitor like 8-azaxanthine crystallizes in the orthorhombic space group I222 with one monomer of 301 residues per subunit. The functional homotetrameric enzyme is built around the 2-fold crystallographic axes. The active site is located at the interface between two subunits folded around a tunnel. 8-azaxanthine is locked in the active site by a Arg 176-Gln 228 molecular tweezers [6,7].

The peroxohole located above the active site is usually filled by a catalytic water molecule W1 hydrogen-bounded to the side

Abbreviation: UOX, urate oxidase

* Corresponding author at: ISTCT UMR 6301, CNRS Université de Caen CEA, centre Cyceron, bd Becquerel, 14074 Caen, France. Tel.: +33 2 31 47 01 32.
E-mail address: colloch@cyceron.fr (N. Colloc'h).

http://dx.doi.org/10.1016/j.febslet.2014.03.017
0014-5793/

chains of Asn 254 and Thr 57* of a symmetric subunit. When UOX crystals are soaked in NaCl or in cyanide solution, the peroxohole exchanges this water molecule for a chloride ion or a cyanide [8,9].

A large internal cavity completely buried inside each monomer is located very close to the active site, with the residue Val 227 in frontier between the active site and the cavity. Indeed, Val 227 side chain lines the internal cavity while its main chain nitrogen is hydrogen-bonded to the ligand (either the inhibitor 8-azaxantine or the natural substrate uric acid). This internal cavity is void, meaning that no water can be seen in the electron density map. It is very hydrophobic, lined with almost 90% of carbon atoms. It is well known that internal cavities within proteins are crucial for conformational flexibility and domain motion [10,11] and accessibility for small ligands can only be granted through thermal motion [12]. Flexibility is thought to be necessary for functional efficiency.

To unravel the functional relevance of UOX internal cavity, we used a structural approach combining crystallography at room temperature under moderate anesthetic gas pressure and under high hydrostatic pressure. These two complementary approaches allow to determine the most flexible part of the protein in relation with internal cavity modifications. Indeed, the analysis of protein structures determined under moderate inert gas pressure have revealed that the main gas-induced structural modifications occur on the volume of cavities which bind the inert gas, their volumes expanding with the applied gas pressure [13,14]. On the other hand, the analysis of protein structures determined under high hydrostatic pressure have revealed that the main pressure-induced structural effects occur on the volumes of cavities which are reduced [15,16]. Activity assays in presence of inert gas and under high hydrostatic pressure have also been performed on UOX to establish the biological significance of these crystallographic findings. We also used crystallography under dioxygen pressure in order to visualize the oxygen binding site.

2. Methods

2.1. Crystallization and data collections

Purified recombinant UOX from *A. flavus*, expressed in *Saccharomyces cerevisiae*, was a gift from Sanofi-Aventis (Montpellier, France). UOX crystals were grown either by batch and hanging-drop methods using a 10–15 mg/ml solution of UOX, with an excess of 8-azaxanthine (purchased from Sigma–Aldrich, Lyon, France), in 50 mM Tris/acetate (pH 8) in the presence of 5–8% PEG 8000. This led to crystal in space group I222 with 1 monomer per asymmetric unit [7].

Crystallography under Xe and N_2O pressure and activity assays in presence of gas have been described in [17]. Crystallography under O_2 pressure has been described in [8] and uses the same experimental devices. Crystallography under high hydrostatic pressure and activity assays under high pressure have been described in [18]. All diffraction data (gas-less, under pressurized gas, ambient pressure and high hydrostatic pressure) have been collected at room temperature.

Diffraction data for two additional structures of UOX in complex with 8-azaxanthin, gas-less and under 4 MPa of dioxygen, were collected at room temperature at the BM14 beamline at the European Synchrotron Radiation facility (ESRF, Grenoble, France). Detector used was a MAR CCD detector. Data were indexed and integrated by *DENZO* and scaled independently and reduced using *SCALEPACK*, both programs from the HKL package [19]. Intensities were converted in structure factor amplitudes using *TRUNCATE* and structure refinements were carried out using *REFMAC* [20], all from the CCP4 package [21]. PDB entry 2IBA in which heteroatoms and alternate side-chain positions were removed was used as starting model for rigid body refinement. The graphics program *COOT* [22] was used to visualize electron density maps and for manual rebuilding. A summary of the X-ray data collection and refinement statistics is given in Table 1. Atomic coordinates and structure factors have been deposited at the PDB (entry code 4OP9 for gas-less UOX and 4OP6 for UOX under 4 MPa oxygen).

Table 1
Data collection and refinement statistics.

	Native	O_2 4 MPa
PDB entry	4OP9	4OP6
Parameters (Å)		
a	80.11	79.92
b	96.18	96.17
c	105.41	105.40
Resolution (Å)	1.60	1.65
Completeness (%)	98.8 (95.6)	100 (100)
Redundancy	5 (4.6)	5 (5)
Unique reflections	55375 (2674)	49104 (2417)
Rsym*	4.2 (36.4)	4.4 (37.3)
I/σ (I)	33.4 (2.9)	33.6 (3.4)
Rwork§	16.78	16.46
Rfree#	19.06	18.85
Mean B factor (Å^2)	22.78	22.62
r.m.s. ideality		
Length (Å)	0.009	0.009
Angle (°)	1.342	1.361

Data between parentheses correspond to the highest resolution shell. *Rsym = $\sum h,k,l \sum i|Ii(h,k,l) - \langle Ii(h,k,l)\rangle|/\sum h,k,l \sum i\ Ii(h,k,l)$, where $Ii(h,k,l)$ is the intensity of observed reflections and $\langle Ii\ (h,k,l)\rangle$ the weighted mean of all observations after rejection of outliers. §Rwork = $\sum|Fo| - |Fc|/\sum|Fo|$; indicates accuracy of the model. #Rfree is a cross validation residual using 5% of the native data which were randomly chosen and excluded from the refinement.

2.2. Cavity volumes calculations

Several programs are available for that purpose, they give slightly different results as the method is very sensitive to the geometric parameters but whatever the program in use, accurate comparative results are obtained as long as the same protocol is used throughout. In the present study, calculations of cavities volume were performed using *CASTp* with a sphere radius of 1.4 Å [23], and *VOIDOO* [24] with the parameters as described in [25]: primary grid spacing of 0.6 Å, grid spacing of 0.6 Å, and probe radius of 1 Å. The cavities volume in the different structures are given in Table 2. Room mean squares deviations (rmsd's) derived from bond lengths, angles, and chiral volumes rmsd's obtained from X-ray structures were found in all cases within the range 5–8% of the calculated volumes. Figures were prepared using *PYMOL* (DeLano Scientific, CA, USA).

3. Results

3.1. Crystallography and activity assays under inert gas pressure

Metabolically inert gases like Xe or N_2O were bound within the internal void cavity of UOX located close to the active site. The main structural modification in UOX-gas complexes was the expansion of the volume of the cavity, which increased with the applied pressure (Fig. 1A). The volume of the internal cavity in the gas-less UOX structure expanded with the presence of gas. The expansion induced by the mixture Xe:N_2O was greater than the expansion induced by Xe alone, itself greater than the expansion induced by N_2O alone (Table 2). In parallel, activity assays performed in presence of air, Xe, N_2O and Xe:N_2O in physiological conditions showed that the presence of gas within the internal

Table 2
Volume (in Å^3) of the internal cavity of urate oxidase in the different PDB files, calculated by *CASTp* or *VOIDOO*.

PDB	4OP9 Native	2ZKA O2 1 MPa	3CKS O2 4 MPa	4OP6 O2 4 MPa	2FUB 140 MPa	3F2M 150 MPa	3PJK Xe 1 MPa	3PKG Xe 2 MPa	3PK4 Xe 3 MPa	3PKU N2O 1 MPa	3PKT N2O 2 MPa	3PK3 N2O 3 MPa	3PLG XeN2O 1 MPa	3PLM XeN2O 2 MPa	3PLJ XeN2O 3 MPa
CASTp	116	150	158	154	102	88	164	168	182	162	166	171	165	180	183
VOIDOO	115	123	127	123	99	103	138	145	145	131	142	143	145	147	147

cavity induced an inhibition of the catalytic reaction. The inhibition induced by the mixture Xe:N_2O was greater than the inhibition induced by Xe alone, itself greater than the inhibition induced by N_2O alone. The correlation between gas-induced structural modifications and gas-induced functional modifications suggested that the cavity has a functional role in the catalytic mechanism of UOX [17].

3.2. Crystallography and activity assays under high hydrostatic pressure

The main structural difference between the crystallographic structures of UOX at 140 or 150 MPa compared to ambient pressure structure was, as expected, the diminution of the volume of the internal cavity (Table 2). Interestingly, the volume of the nearby active site located between two monomers was enlarged by pressure (Fig. 1B). In parallel, activity assays have been performed under pressure. Pressure induced an inhibition of the enzymatic activity of UOX which occurred before the enzyme loose its solubility, meaning that the enzyme was still folded but less active under pressure up to 200 MPa. Above 200 MPa, the protein was then progressively unfolded. The reduction of the cavity volume by pressure in parallel to the increase of the active site volume suggested that the cavity could act as a connecting vessel during the catalytic mechanism [18].

3.3. Crystallography under dioxygen pressure

When using dioxygen under pressure, the gas molecule was observed bound in the active site above the 8-azaxanthine inhibitor [8]. It took the place of the catalytic water molecule W1 in the peroxohole, also interacting with the side chains of Asn 254 and Thr 57* (Fig. 2). When looking at the hydrophobic cavity, no density was visible in the electron density map. However, the volume of the cavity expanded in presence of oxygen (Table 2). This result indicated that, even if no dioxygen molecule was structurally ordered (visible) within the cavity, it would expand its volume. These findings suggested that the cavity might act a transient reservoir for oxygen on its way to the nearby active site.

4. Discussion

In urate oxidase, the internal cavity's volume is modified by pressure and gas presence (Xe, N_2O, XeN_2O and O_2). This modification of volume arises from small perturbations in the residues lining the cavity. To correlate the cavity expansion/reduction and dynamics, we analyzed the isotropic thermal factors of atoms lining the cavity. The average B-factors of the residues lining the cavity and the active site are lower by ~4 Å^2 and by ~3 Å^2 respectively, compared to the overall <B> factors, whatever the analyzed structure (native, high hydrostatic pressure, under Xe, N_2O, XeN_2O or O_2 pressure). Hydrostatic pressure increases the <B> factors by ~5 Å^2, with a similar increase of <B> factors in residues lining the cavity or the active site. The proposed rigidity of the cavity induced by high pressure or gas presence has thus no real incidence on the B-factors of the residues lining it. The modifications of cavity's volumes induced by pressure or gas presence are small, nevertheless they can be considered as meaningful since on one hand they are consistent with external experimental constraints (decreased by pressure and increased with the applied gas pressure) and on the other hand the differences compared to the volume in gas-less urate oxidase at ambient pressure are above the estimated error on volumes (5–8%). The hydrostatic pressure reduces the volume, as estimated by *CASTp*, by 10–20%; gases which bind within the cavity like Xe or N_2O increased the volume

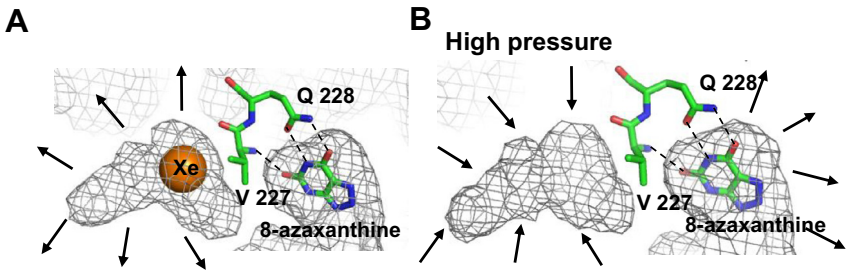

Fig. 1. (A) Active site and its neighboring hydrophobic cavity under 3 MPa of xenon (represented as mesh volumes). Xenon atom is represented by an orange sphere and induces an expansion of the volume of the cavity (represented by arrows). (B) Same representation of the UOX active site and cavity under high hydrostatic pressure. This induces a contraction of the volume of the internal void cavity and an expansion of the volume of the active site located at the interface between two subunits (represented by arrows). The two frontier residues Val 227 and Gln 228 are represented in stick, colored by atom type.

by 40–50%, and gas like O_2 which would be transient in the cavity increased its volume by ~30%.

The structural and functional results presented here highlight that the internal cavity in UOX would play a key role in the enzymatic function. Gas like Xe or N_2O which binds within the nearby cavity induces an expansion of the cavity that inhibits the catalytic mechanism of UOX. On the other hand, high hydrostatic pressure induces a contraction of the cavity and inhibits the catalytic mechanism of UOX. Both gas presence and hydrostatic pressure seems to disrupt the cavity flexibility and increase its rigidity. These results suggest that the cavity rigidity could hamper the active site plasticity, suggesting that, like the active site flexibility, the internal cavity flexibility would be crucial for UOX catalytic activity. The substrate uric acid is flat while the product 5-hydroxyisourate and the intermediate 5-hydroxyperoxoisourate have a larger volume. Thus, the active site needs to expand to accommodate these larger intermediates, a mechanism likely to be hampered when the cavity becomes more rigid.

Proteins possess many conformational sub-states and proteins motions can be described as discrete transitions between numerous conformational sub-states [26,27]. In enzymes, the balance between conformational flexibility and rigidity is adjusted to optimize the catalytic efficiency [28,29]. Energy landscapes of protein can be probed by pressure through the modification of the Gibbs free energy. The pressure modifies the populations of conformers and promote high energy conformers thus allowing the exploration of functional pathways [15,30–34]. Cavities introduce adaptive features that facilitate conformational transitions and are thus thought to play a key role in protein function [35]. In globins for example, cavities are involved in migration pathways for O_2 and CO [36–38]. Mutations that reduce internal cavity volume increase protein stability [39,40]. Anesthetic binding to proteins within internal cavities also leads to an increase in protein stability and further shifts the population of conformational sub-states [41–44]. Pressure can also induce a stabilization through a compression of hydrophobic cavities resulting in increased van der Waals contacts and shifts conformational sub-states [45,46]. Internal cavities play thus a fundamental role in sampling the different conformational sub-states. The present study experimentally illustrates the relationships between local rigidity and overall flexibility, suggesting that UOX cavity would be deeply involved in the protein activity.

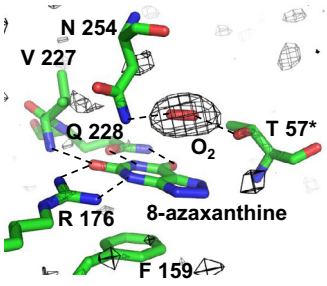

Fig. 2. Electron omit map of the active site of urate oxidase under 4 MPa of dixoygen pressure showing the O_2 molecule in the peroxohole. Residues involved in the catalytic activities are shown in stick, colored by atom type.

Our results also support for the internal cavity of UOX a putative role of a transient docking pathway for dioxygen, since the cavity volume expands in presence of dioxygen. Xenon, which has often been used to probe dioxygen transient pathway, binds within this cavity. For example, in globin and in enzymes, xenon binding sites in cavities map small gaseous ligands transient pathway [38,47–54]. In UOX, the internal cavity where xenon binds is very close to the active site and can have the same function as in globin for dioxygen.

In conclusion, structural and functional analyses of urate oxidase in complex with 8-azaxanthine under inert gas pressure, under dioxygen pressure and under high hydrostatic pressure have suggested a functional relevance of this cavity in the catalytic mechanism. The cavity could be considered as an allosteric site acting as a connecting vessel to give flexibility to the active site, and also as a transient storage place for dioxygen on its way to the peroxohole.

Acknowledgments

The authors gratefully thank Bertrand Castro and Mohamed El Hajji (Sanofi-Aventis, Montpellier, France) for supplying urate oxidase. They also thanks Eric Girard (IBS, Grenoble, France), late Roger Fourme (Synchrotron SOLEIL, France), Beatrice Vallone (La Sapienza University, Rome, Italie), Stéphane Marchal (INSERM, Montpellier, France) and Jacques Abraini (Université de Caen, France) for fruitful and numerous discussions. We also thank Hassan Belrhali, and other members of the staff of the BM14 beamline at ESRF (Grenoble, France) for access and advises. This research was supported by the CNRS, the University of Caen and the University Paris-Descartes.

References

[1] Bongaerts, G.P. and Vogels, G.D. (1979) Mechanism of uricase action. Biochim. Biophys. Acta 567, 295–308.
[2] Bentley, R. and Neuberger, A. (1952) The mechanism of the action of uricase. Biochem. J. 52, 694–699.
[3] Modric, N., Derome, A., Ashcroft, S. and Poje, M. (1992) Tracing and identification of uricase reaction intermediates. Tetrahedron Lett. 33, 6691–6694.
[4] Kahn, K. and Tipton, P.A. (1997) Kinetic mechanism and cofactor content of soybean root nodule urate oxidase. Biochemistry (Mosc.) 36, 4731–4738.
[5] Kahn, K., Serfozo, P. and Tipton, P. (1997) Identification of the true product of the urate oxidase reaction. J. Am. Chem. Soc. 119, 5435–5442.
[6] Colloc'h, N., El Hajji, M., Bachet, B., L'Hermite, G., Schiltz, M., Prangé, T., Castro, B. and Mornon, J.P. (1997) Crystal structure of the protein drug urate oxidase-inhibitor complex at 2.05 Å resolution. Nat. Struct. Biol. 4, 947–952.

[7] Retailleau, P., Colloc'h, N., Vivarès, D., Bonneté, F., Castro, B., El-Hajji, M., Mornon, J.P., Monard, G. and Prangé, T. (2004) Complexed and ligand-free high-resolution structures of urate oxidase (Uox) from *Aspergillus flavus*: a reassignment of the active-site binding mode. Acta Crystallogr. D Biol. Crystallogr. 60, 453–462.

[8] Colloc'h, N., Gabison, L., Monard, G., Altarsha, M., Chiadmi, M., Marassio, G., Sopkova-de Oliveira Santos, J., El Hajji, M., Castro, B., Abraini, J.H. and Prangé, T. (2008) Oxygen pressurized X-ray crystallography: probing the dioxygen binding site in cofactorless urate oxidase and implications for its catalytic mechanism. Biophys. J. 95, 2415–2422.

[9] Gabison, L., Prangé, T., Colloc'h, N., El Hajji, M., Castro, B. and Chiadmi, M. (2008) Structural analysis of urate oxidase in complex with its natural substrate inhibited by cyanide: mechanistic implications. BMC Struct. Biol. 8, 32.

[10] Hubbard, S.J. and Argos, P. (1996) A functional role for protein cavities in domain: domain motions. J. Mol. Biol. 261, 289–300.

[11] Hubbard, S.J., Gross, K.H. and Argos, P. (1994) Intramolecular cavities in globular proteins. Protein Eng. 7, 613–626.

[12] Carugo, O. and Argos, P. (1998) Accessibility to internal cavities and ligand binding sites monitored by protein crystallographic thermal factors. Proteins 31, 201–213.

[13] Prangé, T., Schiltz, M., Pernot, L., Colloc'h, N., Longhi, S., Bourguet, W. and Fourme, R. (1998) Exploring hydrophobic sites in proteins with xenon or krypton. Proteins 30, 61–73.

[14] Quillin, M.L., Breyer, W.A., Griswold, I.J. and Matthews, B.W. (2000) Size versus polarizability in protein-ligand interactions: binding of noble gases within engineered cavities in phage T4 lysozyme. J. Mol. Biol. 302, 955–977.

[15] Fourme, R., Girard, E., Kahn, R., Dhaussy, A.-C. and Ascone, I. (2009) Advances in high-pressure biophysics: status and prospects of macromolecular crystallography. Annu. Rev. Biophys. 38, 153–171.

[16] Girard, E., Kahn, R., Mezouar, M., Dhaussy, A.-C., Lin, T., Johnson, J.E. and Fourme, R. (2005) The first crystal structure of a macromolecular assembly under high pressure: CpMV at 330 MPa. Biophys. J. 88, 3562–3571.

[17] Marassio, G., Prangé, T., David, H.N., Santos, J.S., Gabison, L., Delcroix, N., Abraini, J.H. and Colloc'h, N. (2011) Pressure-response analysis of anesthetic gases xenon and nitrous oxide on urate oxidase: a crystallographic study. Faseb J. 25, 2266–2275.

[18] Girard, E., Marchal, S., Perez, J., Finet, S., Kahn, R., Fourme, R., Marassio, G., Dhaussy, A.-C., Prangé, T., Giffard, M., Dulin, F., Bonneté, F., Lange, R., Abraini, J.H., Mezouar, M. and Colloc'h, N. (2010) Structure-function perturbation and dissociation of tetrameric urate oxidase by high hydrostatic pressure. Biophys. J. 98, 2365–2373.

[19] Otwinowski, Z. and Minor, W. (1997) Processing of X-ray diffraction data collected in the oscillation mode. Methods Enzymol. 276, 307–326.

[20] Murshudov, G.N., Vagin, A.A. and Dodson, E.J. (1997) Refinement of macromolecular structures by the Maximum-Likelihood method. Acta Crystallogr. D Biol. Crystallogr. 53, 240–255.

[21] Collaborative Computational Project 4 (1994) The CCP4 suite : programs for protein crystallography. Acta Crystallogr. D Biol. Crystallogr. 50, 760–763.

[22] Emsley, P. and Cowtan, K. (2004) Coot: model-building tools for molecular graphics. Acta Crystallogr. D Biol. Crystallogr. 60, 2126–2132.

[23] Dundas, J., Ouyang, Z., Tseng, J., Binkowski, A., Turpaz, Y. and Liang, J. (2006) CASTp: computed atlas of surface topography of proteins with structural and topographical mapping of functionally annotated residues. Nucleic Acids Res. 34, W116–118.

[24] Kleywegt, G.J. and Jones, T.A. (1994) Detection, delineation, measurement and display of cavities in macromolecular structures. Acta Crystallogr. D Biol. Crystallogr. 50, 178–185.

[25] Colloc'h, N., Sopkova-de Oliveira Santos, J., Retailleau, P., Vivarès, D., Bonneté, F., Langlois d'Estaintot, B., Gallois, B., Brisson, A., Risso, J.J., Lemaire, M., Prangé, T. and Abraini, J.H. (2007) Protein crystallography under xenon and nitrous oxide pressure: comparison with in vivo pharmacology studies and implications for the mechanism of inhaled anesthetic action. Biophys. J. 92, 217–224.

[26] Frauenfelder, H., Sligar, S.G. and Wolynes, P.G. (1991) The energy landscapes and motions of proteins. Science 254, 1598–1603.

[27] Frauenfelder, H., Fenimore, P.W. and Young, R.D. (2007) Protein dynamics and function: insights from the energy landscape and solvent slaving. IUBMB Life 59, 506–512.

[28] Chiuri, R., Maiorano, G., Rizzello, A., del Mercato, L.L., Cingolani, R., Rinaldi, R., Maffia, M. and Pompa, P.P. (2009) Exploring local flexibility/rigidity in psychrophilic and mesophilic carbonic anhydrases. Biophys. J. 96, 1586–1596.

[29] Tehei, M. and Zaccai, G. (2007) Adaptation to high temperatures through macromolecular dynamics by neutron scattering. FEBS J. 274, 4034–4043.

[30] Akasaka, K. (2006) Probing conformational fluctuation of proteins by pressure perturbation. Chem. Rev. 106, 1814–1835.

[31] Collins, M.D., Kim, C.U. and Gruner, S.M. (2011) High-pressure protein crystallography and NMR to explore protein conformations. Annu. Rev. Biophys. 40, 81–98.

[32] Fourme, R., Girard, E. and Akasaka, K. (2012) High-pressure macromolecular crystallography and NMR: status, achievements and prospects. Curr. Opin. Struct. Biol. 22, 636–642.

[33] Frauenfelder, H., Alberding, N., Ansari, A., Braunstein, D., Cowen, B., Hong, M., Iben, I., Johnson, J., Luck, S., Marden, M., Mourant, J., Ormos, P., Reinisch, L., Scholl, R., Schulte, A., Shyamsunder, E., Sorensen, L., Steinbach, P., Xie, A., Young, R. and Yue, K. (1990) Proteins and pressure. J. Chem. Phys. 94, 1024–1037.

[34] Urayama, P., Phillips Jr., G.N. and Gruner, S.M. (2002) Probing substates in sperm whale myoglobin using high-pressure crystallography. Structure (Lond. Engl. 1993) 10, 51–60.

[35] Lopez, C.J., Yang, Z., Altenbach, C. and Hubbell, W.L. (2013) Conformational selection and adaptation to ligand binding in T4 lysozyme cavity mutants. Proc. Natl. Acad. Sci. U.S.A. 110, E4306–4315.

[36] Bossa, C., Amadei, A., Daidone, I., Anselmi, M., Vallone, B., Brunori, M. and Di Nola, A. (2005) Molecular dynamics simulation of sperm whale myoglobin: effects of mutations and trapped CO on the structure and dynamics of cavities. Biophys. J. 89, 465–474.

[37] Brunori, M. and Gibson, Q.H. (2001) Cavities and packing defects in the structural dynamics of myoglobin. EMBO Rep. 2, 674–679.

[38] Tilton Jr, R.F., Kuntz Jr, I.D. and Petsko, G.A. (1984) Cavities in proteins: structure of a metmyoglobin-xenon complex solved to 1.9 A. Biochemistry (Mosc.) 23, 2849–2857.

[39] Lee, C., Maeng, J.S., Kocher, J.P., Lee, B. and Yu, M.H. (2001) Cavities of alpha(1)-antitrypsin that play structural and functional roles. Protein Sci. Publ. Protein Soc. 10, 1446–1453.

[40] Ogata, K., Kanei-Ishii, C., Sasaki, M., Hatanaka, H., Nagadoi, A., Enari, M., Nakamura, H., Nishimura, Y., Ishii, S. and Sarai, A. (1996) The cavity in the hydrophobic core of Myb DNA-binding domain is reserved for DNA recognition and trans-activation. Nat. Struct. Biol. 3, 178–187.

[41] Eckenhoff, R.G. (2001) Promiscuous ligands and attractive cavities: how do the inhaled anesthetics work ? Mol. Interv. 1, 258–268.

[42] Johansson, J.S., Zou, H. and Tanner, J.W. (1999) Bound volatile general anesthetics alter both local protein dynamics and global protein stability. Anesthesiology 90, 235–245.

[43] Vemparala, S., Domene, C. and Klein, M.L. (2008) Interaction of anesthetics with open and closed conformations of a potassium channel studied via molecular dynamics and normal mode analysis. Biophys. J. 94, 4260–4269.

[44] Vemparala, S., Domene, C. and Klein, M.L. (2010) Computational studies on the interactions of inhalational anesthetics with proteins. Acc. Chem. Res. 43, 103–110.

[45] Boonyaratanakornkit, B.B., Park, C.B. and Clark, D.S. (2002) Pressure effects on intra- and intermolecular interactions within proteins. Biochim. Biophys. Acta 1595, 235–249.

[46] Collins, M.D., Quillin, M.L., Hummer, G., Matthews, B.W. and Gruner, S.M. (2007) Structural rigidity of a large cavity-containing protein revealed by high-pressure crystallography. J. Mol. Biol. 367, 752–763.

[47] Cohen, J., Arkhipov, A., Braun, R. and Schulten, K. (2006) Imaging the migration pathways for O_2, CO, NO, and Xe inside myoglobin. Biophys. J. 91, 1844–1857.

[48] Knapp, J.E., Pahl, R., Cohen, J., Nichols, J.C., Schulten, K., Gibson, Q.H., Srajer, V. and Royer Jr., W.E. (2009) Ligand migration and cavities within Scapharca Dimeric HbI: studies by time-resolved crystallo-graphy, Xe binding, and computational analysis. Structure (Lond. Engl. 1993) 17, 1494–1504.

[49] Moschetti, T., Mueller, U., Schulze, J., Brunori, M. and Vallone, B. (2009) The structure of neuroglobin at high Xe and Kr pressure reveals partial conservation of globin internal cavities. Biophys. J 97, 1700–1708.

[50] De Sanctis, D., Dewilde, S., Pesce, A., Moens, L., Ascenzi, P., Hankeln, T., Burmester, T. and Bolognesi, M. (2004) Mapping protein matrix cavities in human cytoglobin through Xe atom binding. Biochem. Biophys. Res. Commun. 316, 1217–1221.

[51] Savino, C., Miele, A.E., Draghi, F., Johnson, K.A., Sciara, G., Brunori, M. and Vallone, B. (2009) Pattern of cavities in globins: the case of human hemoglobin. Biopolymers 91, 1097–1107.

[52] Duff, A.P., Trambaiolo, D.M., Cohen, A.E., Ellis, P.J., Juda, G.A., Shepard, E.M., Langley, D.B., Dooley, D.M., Freeman, H.C. and Guss, J.M. (2004) Using xenon as a probe for dioxygen-binding sites in copper amine oxidases. J. Mol. Biol. 344, 599–607.

[53] Hiromoto, T., Fujiwara, S., Hosokawa, K. and Yamaguchi, H. (2006) Crystal structure of 3-hydroxybenzoate hydroxylase from Comamonas testosteroni has a large tunnel for substrate and oxygen access to the active site. J. Mol. Biol. 364, 878–896.

[54] Wade, R.C., Winn, P.J., Schlichting, I. and Sudarko (2004) A survey of active site access channels in cytochromes P450. J. Inorg. Biochem. 98, 1175–1182.